

CT Angiography of Pulmonary Embolism: Diagnostic Criteria and Causes of Misdiagnosis¹

CME FEATURE

See accompanying test at http://www.rsna.org/education/lrg_cme.html

LEARNING OBJECTIVES FOR TEST 1

After reading this article and taking the test, the reader will be able to:

- List the diagnostic criteria for acute and chronic pulmonary embolism at CT pulmonary angiography.
- Describe the causes of misdiagnosis of pulmonary embolism at CT pulmonary angiography.
- Discuss the causes of indeterminate CT pulmonary angiography.

Conrad Wittram, MB, ChB • Michael M. Maher, MD • Albert J. Yoo, MD
Mannudeep K. Kalra, MD • Jo-Anne O. Shepard, MD
Theresa C. McLoud, MD

Computed tomographic (CT) pulmonary angiography is becoming the standard of care at many institutions for the evaluation of patients with suspected pulmonary embolism. This pathologic condition, whether acute or chronic, causes both partial and complete intraluminal filling defects, which should have a sharp interface with intravascular contrast material. In acute pulmonary embolism that manifests as complete arterial occlusion, the affected artery may be enlarged. Partial filling defects due to acute pulmonary embolism are often centrally located, but when eccentrically located they form acute angles with the vessel wall. Chronic pulmonary embolism can manifest as complete occlusive disease in vessels that are smaller than adjacent patent vessels. Other CT pulmonary angiographic findings in chronic pulmonary embolism include evidence of recanalization, webs or flaps, and partial filling defects that form obtuse angles with the vessel wall. Factors that cause misdiagnosis of pulmonary embolism may be patient related, technical, anatomic, or pathologic. The radiologist needs to determine the quality of a CT pulmonary angiographic study and whether pulmonary embolism is present. If the quality of the study is poor, the radiologist should identify which pulmonary arteries have been rendered indeterminate and whether additional imaging is necessary.

©RSNA, 2004

Index terms: Computed tomography (CT), angiography, 94.12916 • Embolism, pulmonary, 94.77 • Pulmonary angiography, 94.12916 • Pulmonary arteries, CT, 94.12916 • Pulmonary arteries, stenosis or obstruction, 94.77

RadioGraphics 2004; 24:1219–1238 • Published online 10.1148/rg.245045008 • Content Codes: **CA** **CH** **CT**

¹From the Department of Radiology, Massachusetts General Hospital and Harvard Medical School, Founders Building 202, 55 Fruit St, Boston, MA 02114. Recipient of a Certificate of Merit award for an education exhibit at the 2003 RSNA scientific assembly. Received January 13, 2004; revision requested March 10 and received April 16; accepted April 16. All authors have no financial relationships to disclose. Address correspondence to C.W. (e-mail: cwittram@partners.org).

©RSNA, 2004

Protocol for 16-Section CT of Pulmonary Embolism

Parameter	Normal-sized Patients	Large Patients (>250 lb)
Detector width (mm)	1.25	2.5
Reconstruction interval (mm)	0.625	1.25
Table movement (mm per rotation)	13.75	6.88
Pitch	1.375:1	0.562:1
Peak voltage (kVp)	120	140
Tube current (mAs)	Maximum	Maximum
Rotation time (sec)	0.5	0.5
Contrast material injection		
Volume (mL)	135	135
Rate (mL/sec)	4	4
Scanning delay*	Variable	Variable

*Scanning delay is determined by dividing the acquisition time for lung imaging by 2 and subtracting the result from the total injection time (34 seconds). Thus, for example, with an acquisition time of 10 seconds, the scanning delay will be 34 seconds – 5 seconds, or 29 seconds. No timing bolus is necessary unless the patient has a known history of heart disease.

Introduction

Pulmonary embolism is the third most common acute cardiovascular disease after myocardial infarction and stroke and results in thousands of deaths each year because it often goes undetected (1,2). Diagnostic tests for thromboembolic disease include (a) the D-dimer assay, which has a high sensitivity but poor specificity in this setting (3), (b) ventilation-perfusion scintigraphy, which has a high sensitivity but very poor specificity (4), and (c) lower limb ultrasonography, which has a high specificity but low sensitivity (5). Computed tomographic (CT) pulmonary angiography has been evaluated with meta-analysis and has demonstrated sensitivities of 53%–100% and specificities of 83%–100% (6), wide ranges that are explained in part by technologic improvements over time. Pulmonary angiography, the diagnostic standard of reference for confirming or refuting a diagnosis of pulmonary embolism, remains underused (7,8). Although pulmonary angiography has lower mortality and morbidity rates (<1% and 5%, respectively) than anticoagulation therapy (1%–2% and 5%–25%), it has not gained widespread acceptance and is not universally available (9–11). In a study evaluating trends in the use of inpatient thoracic radiology at an academic medical center over a 10-year period, Wittram et al (12) showed that the use of CT in patients with suspected thromboembolic disease has increased significantly (Figs 1–3) (12).

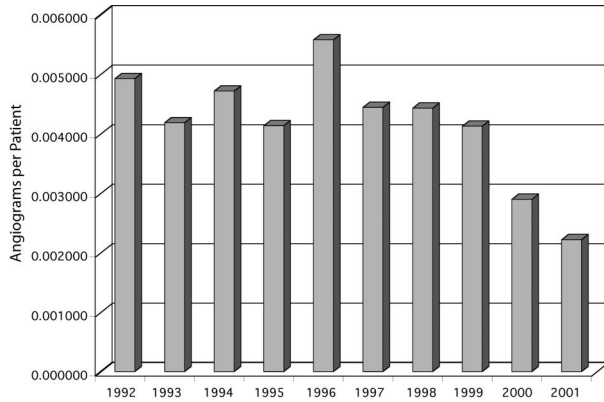
In this article, we describe the technique of CT pulmonary angiography, diagnostic criteria for acute and chronic pulmonary embolism, and causes of misdiagnosis of pulmonary embolism.

The latter group includes patient-related factors (respiratory motion artifact, image noise, pulmonary artery catheter, flow-related artifact), technical factors (window settings, streak artifact, lung algorithm artifact, partial volume artifact, stair step artifact), anatomic factors (partial volume averaging effect in lymph nodes, vascular bifurcation, misidentification of veins), and pathologic factors (mucus plug, perivascular edema, localized increase in vascular resistance, pulmonary artery stump in situ thrombosis, primary pulmonary artery sarcoma, tumor emboli).

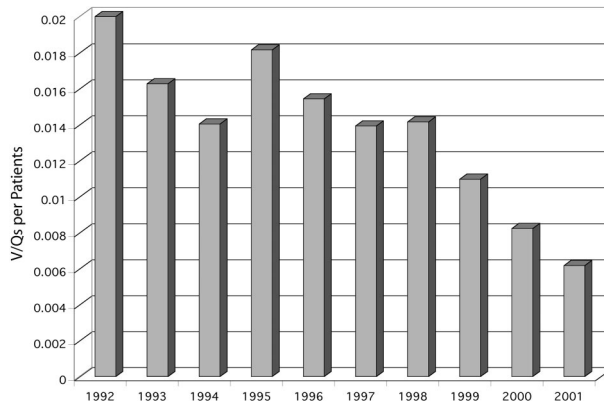
CT Technique

Lightspeed 16-section CT scanners (GE Medical Systems, Milwaukee, Wis) are used to acquire images of the thorax in a caudocranial direction. For intravenous access, introduction of an 18- or 20-gauge catheter into an antecubital vein is preferred. The chest field of view is the widest rib-to-rib distance acquired during breath hold after inspiration. Images are acquired with a standard algorithm and viewed with IMPAX version 4.1 software (AGFA, Teterboro, NJ). Our CT techniques are shown in the Table. Images are displayed with three different gray scales for interpretation of lung window (window width/level [HU] = 1500/600), mediastinal window (400/40), and pulmonary embolism-specific (700/100) settings. Multiplanar reformatted images through the longitudinal axis of a vessel are sometimes used to overcome various difficulties encountered with axial sections of obliquely or axially oriented arteries (13). Reformatted images can help differentiate between true pulmonary embolism and a variety of patient-related, technical, anatomic, and pathologic factors that can mimic pulmonary embolism.

Figures 1–3. (1) Graph illustrates that the number of pulmonary angiographic studies performed per inpatient with suspected thromboembolic disease decreased significantly between 1992 and 2001 ($P = .02$). (2) Graph illustrates that the number of ventilation-perfusion scans performed per inpatient with suspected thromboembolic disease decreased significantly between 1992 and 2001 ($P = .0003$). (3) Graph illustrates that the number of CT studies performed for pulmonary embolism per inpatient increased significantly between 1992 and 2001 ($P = .006$). Figures 1–3 demonstrate the timing of changes that occur when a new technology replaces an old one; in this case, a downturn in the use of pulmonary angiography and ventilation-perfusion scintigraphy almost exactly coincides with a steep increase in CT pulmonary angiography usage. (Fig 1 modified and Figs 1–3 reprinted, with permission, from reference 12.)



1.

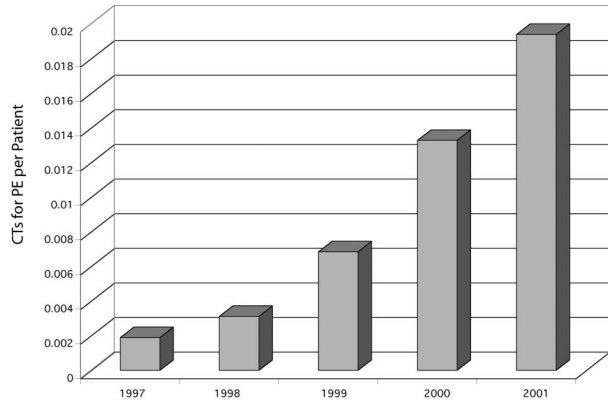


2.

Contrast material–enhanced spiral CT of the veins of the lower extremities is performed with the same contrast material bolus that is used for chest CT. Images of the iliac, femoral, and popliteal veins are obtained 4 minutes after the onset of enhancement from the initial contrast material injection. Multisection CT venography is simple and accurate, and when combined with lung imaging it allows fast and comprehensive evaluation for thromboembolic disease (14).

Diagnostic Criteria for Pulmonary Embolism

For each lung, the main, lobar, segmental, and subsegmental arteries are examined for pulmonary embolism. Both acute and chronic pulmonary embolism cause intraluminal filling defects that should have a sharp interface with the intravascular contrast material. The vessels are seen as



3.

either normal, containing acute pulmonary embolism, containing chronic pulmonary embolism, or indeterminate. The reason for indeterminacy is reported, along with the extent of normalcy. For example, vessels may appear normal to the level of the segmental arteries; however, the presence of pulmonary embolism in subsegmental arteries may remain indeterminate depending on the quality of the study.

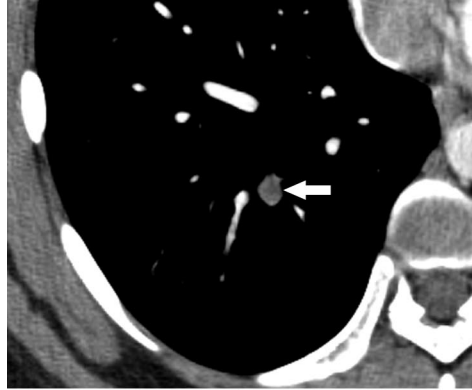
Acute Pulmonary Embolism

The diagnostic criteria for acute pulmonary embolism include the following:

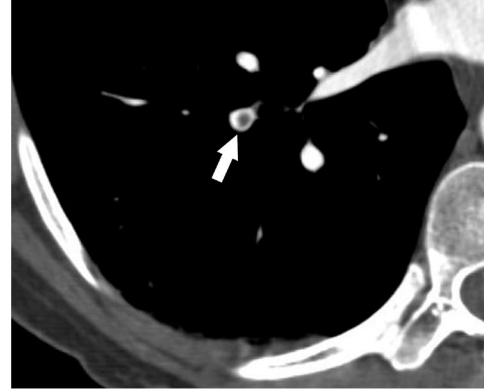
1. Arterial occlusion with failure to enhance the entire lumen due to a large filling defect; the artery may be enlarged compared with adjacent patent vessels (Fig 4).
2. A partial filling defect surrounded by contrast material, producing the “polo mint” sign on images acquired perpendicular to the long axis of a vessel (Fig 5) and the “railway track” sign on longitudinal images of the vessel (Fig 6).
3. A peripheral intraluminal filling defect that forms acute angles with the arterial wall (Fig 7) (15–17).

Peripheral wedge-shaped areas of hyperattenuation that may represent infarcts, along with linear bands, have been demonstrated to be statistically significant ancillary findings associated with

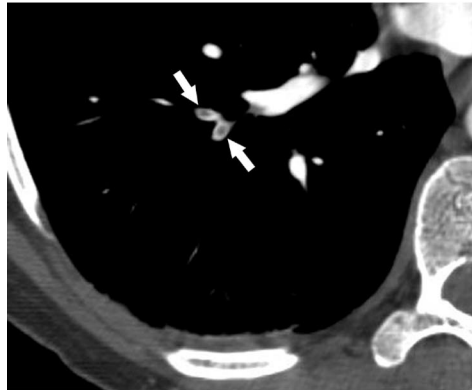
Figures 4–6. (4) Acute occlusive pulmonary embolism in a 32-year-old woman who presented with chest pain. CT scan shows a pulmonary embolus within the posterobasal segment of the right lower lobe artery (arrow). The artery is enlarged compared with adjacent patent vessels. (5) Acute pulmonary embolism in a 45-year-old woman who presented with chest pain. (a) CT scan shows a pulmonary embolus that affects the segmental artery of the laterobasal segment of the right lower lobe. This partial filling defect surrounded by contrast material produces the polo mint sign (arrow). (b) CT scan shows acute emboli that affect subsegmental arteries of the laterobasal segment (arrows). (6) Acute pulmonary embolism in a 66-year-old man who presented with chest pain and dyspnea. CT scan shows an acute pulmonary embolus that causes a partial filling defect surrounded by contrast material (railway track sign) (arrow). Another acute pulmonary embolus affects the left main pulmonary artery (arrowhead).



4.



5a.

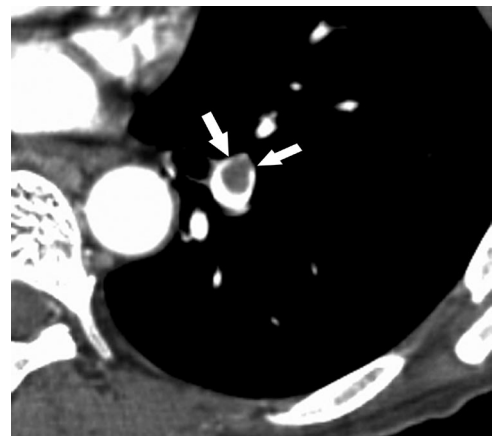


5b.



6.

Figure 7. Acute pulmonary embolism in a 58-year-old woman who presented with chest pain and dyspnea. CT scan demonstrates a pulmonary embolus that results in an eccentrically positioned partial filling defect, which is surrounded by contrast material and forms acute angles with the arterial wall (arrows).



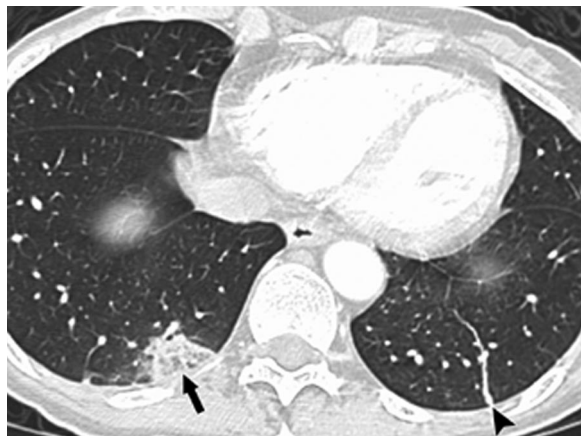


Figure 8. Acute pulmonary embolism in a 58-year-old woman who presented with chest pain and dyspnea. CT scan shows an acute pulmonary embolus with ancillary findings of a peripheral wedge-shaped area of hyperattenuation in the lung (arrow), a finding that may represent an infarct, as well as a linear band (arrowhead).

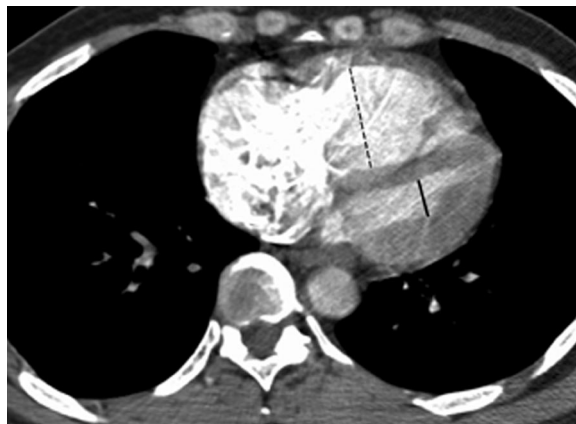
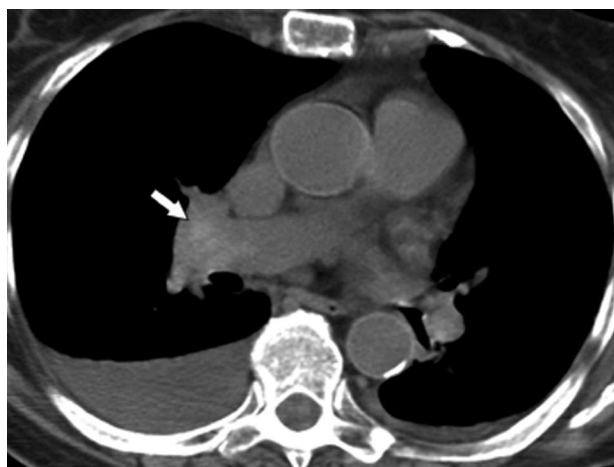


Figure 9. Acute pulmonary embolism in a 42-year-old man who presented with chest pain and severe dyspnea. CT scan reveals that the short axis of the right ventricle (dashed line) is wider than that of the left ventricle (solid line), a situation that was caused by acute pulmonary embolism and created right ventricular strain.



a.



b.

Figure 10. Acute central pulmonary embolism in an asymptomatic 87-year-old woman. **(a)** Unenhanced CT scan demonstrates subtle regions of hyperattenuation (arrow). **(b)** Confirmatory CT pulmonary angiogram demonstrates acute pulmonary embolism within the right main and left interlobar pulmonary arteries.

acute pulmonary embolism (Fig 8) (18). However, these radiologic features are not specific for pulmonary embolism. If findings in the pulmonary arteries are indeterminate and the lungs are clear, ventilation-perfusion scintigraphy may be performed. Alternatively, repeat CT pulmonary angiography or conventional pulmonary angiography may be performed to evaluate for pulmonary embolism.

After experiencing an initial embolic event, a patient may be at risk for circulatory collapse secondary to right-sided heart failure, and a subsequent embolism may be fatal. Early detection of acute right ventricular failure allows implementation of the most appropriate therapeutic strategy. Right ventricular strain or failure is optimally monitored with echocardiography. However, some morphologic abnormalities that suggest

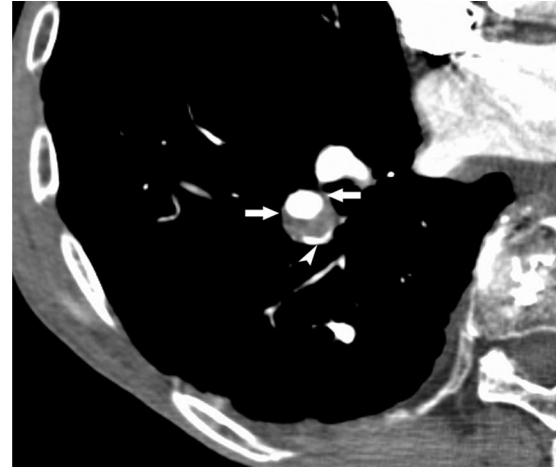
right ventricular failure can be quantified with CT pulmonary angiography. These CT findings include *(a)* right ventricular dilatation (in which the right ventricular cavity is wider than the left ventricular cavity in the short axis) (Fig 9) (19), with or without contrast material reflux into the hepatic veins; *(b)* deviation of the interventricular septum toward the left ventricle (Fig 9) (19); or *(c)* a pulmonary embolism index greater than 60% (20).

Pulmonary emboli have been identified on 1.5% of contrast-enhanced CT scans obtained for reasons other than evaluation for pulmonary embolism (21). In addition, a centrally located, hyperattenuating filling defect is occasionally identified at unenhanced CT, a finding that indicates acute central pulmonary embolism (Fig 10) (22).

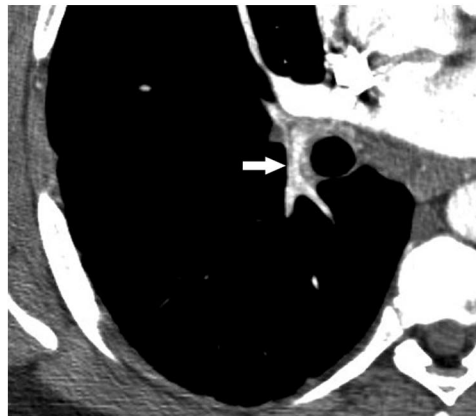
Figures 11–14. (11) Chronic pulmonary embolism in a 27-year-old man with dyspnea. CT scan shows complete occlusion of vessels in the left lung (arrowheads) that are smaller than adjacent patent vessels. Note the collateral blood supply from a branch of the right hemidiaphragmatic artery (arrow). (12) Chronic pulmonary embolism in a 62-year-old man with dyspnea. CT scan shows an eccentrically located thrombus that forms obtuse angles with the vessel wall (arrows). Note the dilated collateral bronchial artery (arrowhead). (13) Chronic pulmonary embolism in the same patient as in Figure 11. CT scan reveals a small, recanalized pulmonary artery with contrast material in the central lumen (arrow). (14) Chronic pulmonary embolism in a 56-year-old man with dyspnea. CT scan shows a flap (arrow) within a small right interlobar pulmonary artery. Collateral bronchial artery dilatation is also noted (arrowhead).



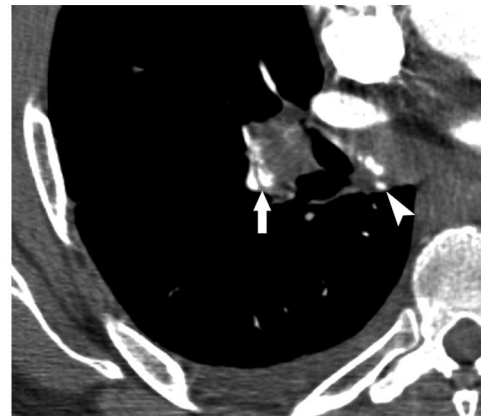
11.



12.



13.



14.

These are important observations because acute pulmonary embolism may be identified even if it is not suspected clinically. Such detection can help determine further imaging needs and allow the timely initiation of appropriate therapy.

CT pulmonary angiography can help identify diseases that have symptoms similar to those of acute pulmonary embolism. The more common diseases that can be detected with CT include pericarditis, which may manifest as pericardial thickening or fluid; acute myocardial infarction, which may manifest as a filling defect within a

coronary artery or as a perfusion defect of the myocardium; and aortic dissection. Esophagitis and, rarely, esophageal rupture may also be identified, as well as pneumonia, lung cancer, and pleural disease, including pneumothorax and pleuritis. Chest wall abnormalities such as rib fractures and metastatic deposits may also mimic pulmonary embolism.

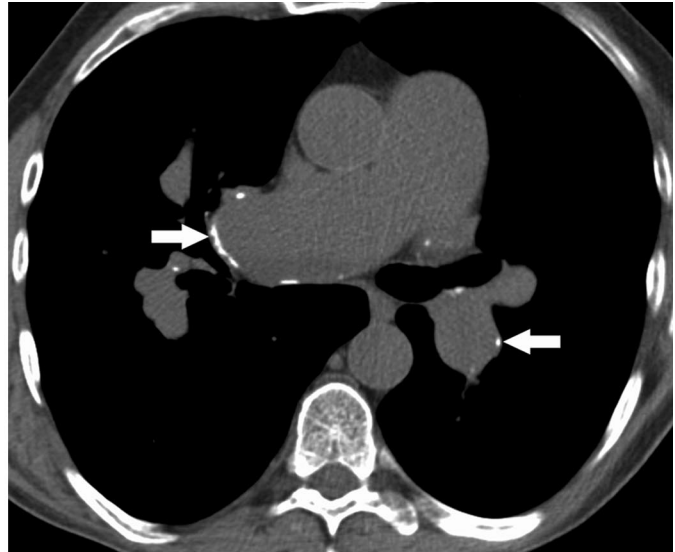
Chronic Pulmonary Embolism

The diagnostic criteria for chronic pulmonary embolism include (a) complete occlusion of a vessel that is smaller than adjacent patent vessels (Fig 11); (b) a peripheral, crescent-shaped intraluminal defect that forms obtuse angles with

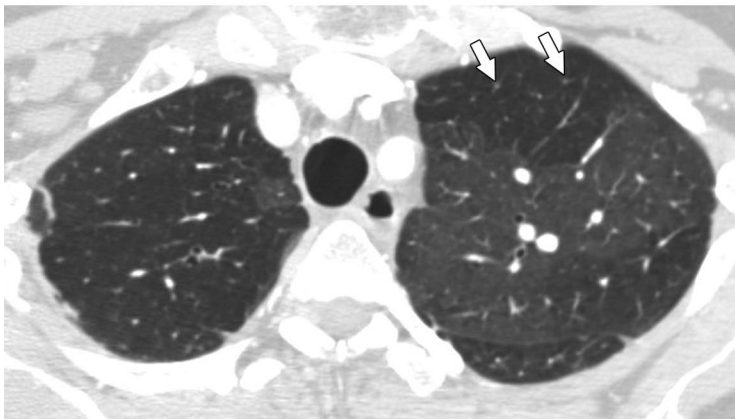
Figures 15–17. (15) Chronic pulmonary embolism in the same patient as in Figure 12. CT scan shows a large chronic pulmonary embolus in the main and left main pulmonary arteries (arrowhead). Arrows indicate collateral bronchial arteries. (16) Chronic pulmonary embolism in a 60-year-old woman with dyspnea. CT scan demonstrates a mosaic perfusion pattern. The dark regions of underperfused lung are seen to contain vessels (arrows) that are smaller than the adjacent patent vessels in the normally perfused lung. (17) Chronic pulmonary embolism in a 62-year-old man with dyspnea. CT scan shows pulmonary arterial wall calcification (arrows), a secondary sign of chronic pulmonary embolism.



15.



17.



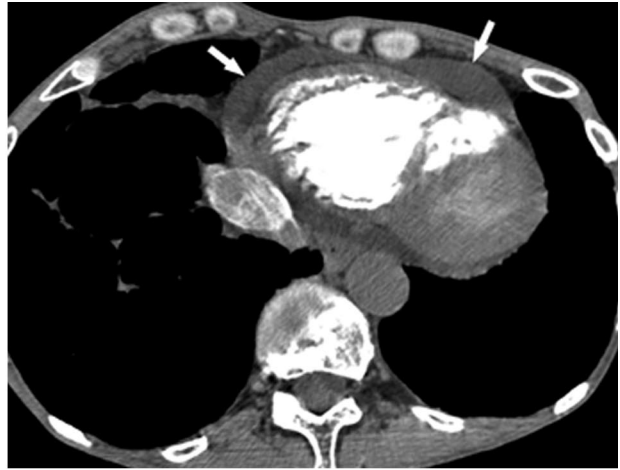
16.

the vessel wall (Fig 12); (c) contrast material flowing through thickened, often smaller arteries due to recanalization (Fig 13); (d) a web or flap within a contrast material-filled artery (Fig 14); and (e) secondary signs, including extensive bronchial or other systemic collateral vessels (Figs 11, 12, 14, 15), an accompanying mosaic perfusion pattern (Fig 16), or calcification within eccentric vessel thickening (Fig 17) (15,17).

Ancillary findings in chronic pulmonary embolism may include CT changes caused by pulmonary arterial hypertension: a pulmonary artery diameter greater than 33 mm (Fig 18) (23) and pericardial fluid (Fig 19) (24).



18.



19.

Figures 18, 19. (18) Pulmonary arterial hypertension secondary to chronic pulmonary embolism in the same patient as in Figure 12. On a CT scan, the pulmonary artery measures 41 mm in diameter (black line), a finding that indicates hypertension. (19) Chronic pulmonary embolism in the same patient as in Figure 12. CT scan demonstrates pericardial fluid (arrows) associated with pulmonary arterial hypertension secondary to chronic pulmonary embolism.



a.

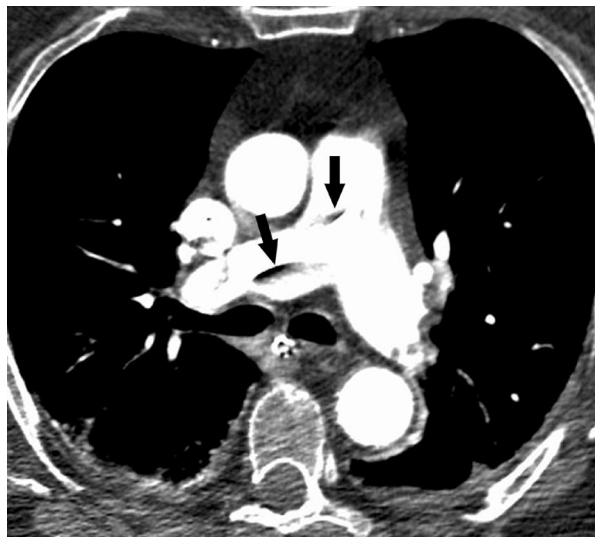


b.

Figure 20. Respiratory motion artifact in a 61-year-old man with dyspnea. (a) CT scan (lung window) shows composite images of vessels (seagull sign) (arrows). (b) CT scan (mediastinal window) demonstrates a low-attenuation abnormality caused by partial volume averaging of vessel and adjacent lung (arrow), a finding that can simulate pulmonary embolism.

Figure 21. Image noise in scans of a 39-year-old woman with chest pain. CT scan clearly depicts image noise pixels within the contrast material–filled heart chambers, a confluence of which could be misinterpreted as pulmonary embolism (arrow). Unlike true emboli, however, these apparent abnormalities are not well-defined filling defects. Small pulmonary emboli could be obscured by a large amount of image noise.





a.



b.

Figure 22. Beam-hardening artifact in a 63-year-old man with respiratory failure. **(a)** On a CT scan, a pulmonary artery catheter causes adjacent beam-hardening artifacts within the main and right pulmonary arteries that mimic pulmonary embolism (arrows). Small pulmonary emboli are noted in the left pulmonary artery. **(b)** CT scan produced with bone window settings clearly depicts the pulmonary artery catheter. Adjacent beam-hardening artifacts are also seen.

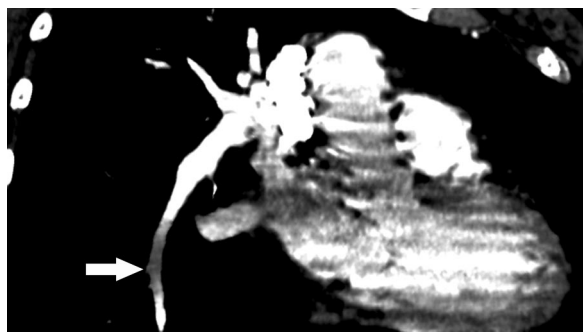


Figure 23. Flow-related artifact in a 60-year-old woman with pleuritic chest pain. Coronal reformatted image of the right interlobar artery and the posterobasal segment of the pulmonary artery demonstrates dense contrast material superior and inferior to a region of poorly enhanced blood (arrow).

Causes of Misdiagnosis of Pulmonary Embolism

Patient-related Factors

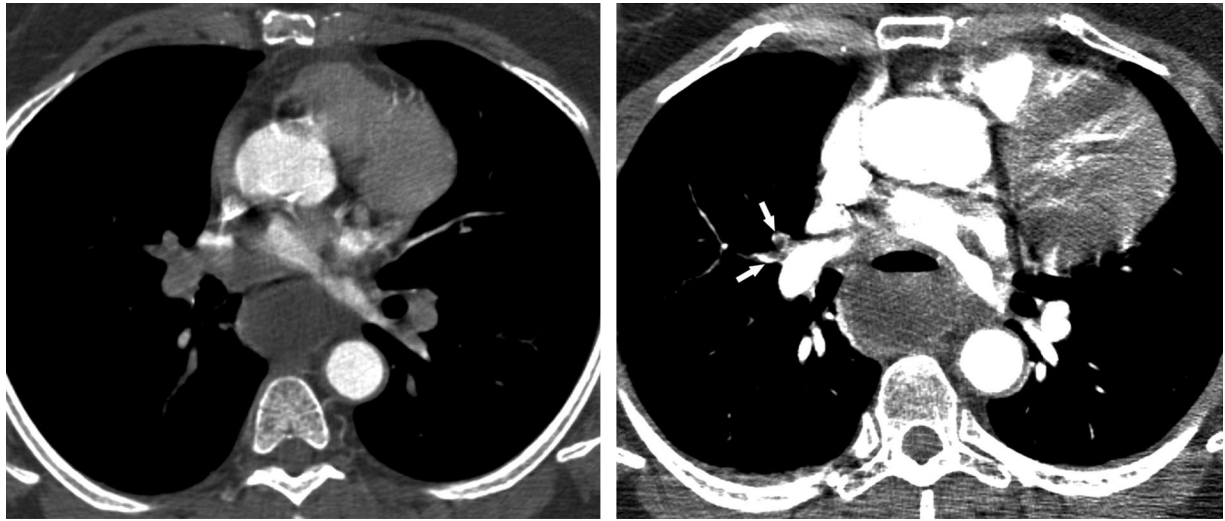
Respiratory Motion Artifact.—Respiratory motion artifacts are the most common cause of indeterminate CT pulmonary angiography and can cause misdiagnosis of pulmonary embolism. These artifacts are best seen with lung window settings and can create the “seagull” sign (Fig 20a). Rapid change in the position of vessels on contiguous images also confirms motion artifact. The low-attenuation abnormality due to partial volume averaging of vessel and lung can simulate pulmonary embolism (Fig 20b). Motion artifact renders the diagnosis of pulmonary embolism at this anatomic level indeterminate. Respiratory motion artifact will diminish as higher-order multisection CT, which requires a shorter breath hold, becomes more widely used.

Image Noise.—Images obtained in large patients have more quantum mottle. Image noise

makes the evaluation of segmental and subsegmental vessels difficult and can cause indeterminate CT pulmonary angiography and misdiagnosis of pulmonary embolism (Fig 21). Therefore, for patients weighing more than 250 pounds, we modify our protocol by increasing detector width to 2.5 mm, thereby decreasing image noise and improving scan quality. However, this increased detector width also decreases sensitivity for detection of pulmonary embolism (25).

Pulmonary Artery Catheter.—A pulmonary artery catheter that is being used for invasive hemodynamic monitoring of critically ill patients can cause beam-hardening artifacts or may itself mimic pulmonary embolism (Fig 22) (26). Identification of the catheter with bone window settings (Fig 22) or on contiguous images or the scout image will demonstrate the true nature of this pitfall.

Flow-related Artifact.—Bilateral lower lobe flow-related artifacts due to poor mixture of blood and contrast material can cause transient interruption of contrast enhancement (Fig 23), which can in turn lead to indeterminate CT



a.

b.

Figure 24. Flow-related artifact in a 73-year-old woman with chest pain. (a) CT scan shows poor enhancement of the interlobar and middle lobe pulmonary arteries due to flow-related artifact. More distally, the pulmonary arteries were well enhanced. Note also the fluid-filled, dilated esophagus. (b) Repeat CT pulmonary angiogram demonstrates segmental pulmonary emboli within the medial and lateral segmental branches of the middle lobe artery (arrows).

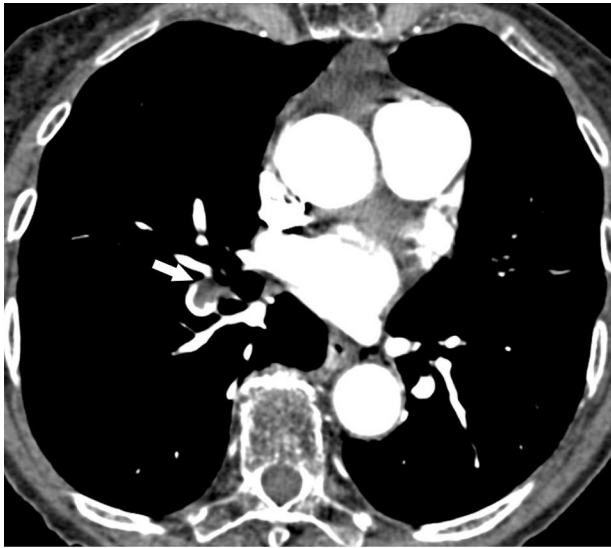
pulmonary angiography and misdiagnosis of pulmonary embolism. Transient interruption of contrast enhancement is likely related to inspiration and to unenhanced blood entering the right atrium, right ventricle, and pulmonary arteries from the inferior vena cava just prior to image acquisition (27). A flow-related artifact can be confidently diagnosed by identifying its ill-defined margins and by demonstrating an attenuation level above 78 HU (28). However, further imaging may be necessary to exclude thrombus hidden in poorly enhanced vessels (Fig 24). As CT scanners become faster, delaying initial image acquisition until approximately 5 seconds after inspiration should allow the transient interruption in contrast material to pass through the pulmonary circulation (27).

Technical Factors

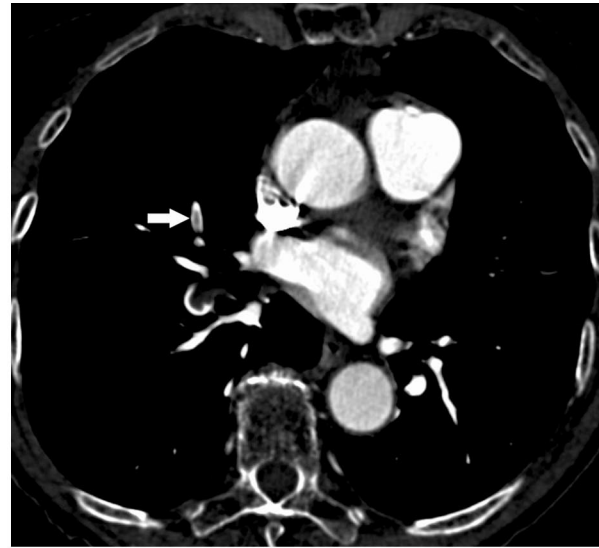
Window Settings.—The appropriate window width and level settings are important for identify-

ing small emboli, webs, or flaps. Very bright vessel contrast can obscure small pulmonary emboli. Brink et al (29) suggested a window width equal to the measured mean attenuation of the enhanced main pulmonary artery plus two standard deviations and a window level equal to one-half of this value (Fig 25). We use pulmonary embolism-specific settings with a window width and level of 700 and 100 HU, respectively (Fig 25c). This approach helps differentiate between a sharply marginated embolus and an ill-defined artifact. However, these modified window settings can also increase the conspicuity of artifacts caused by image noise and flow.

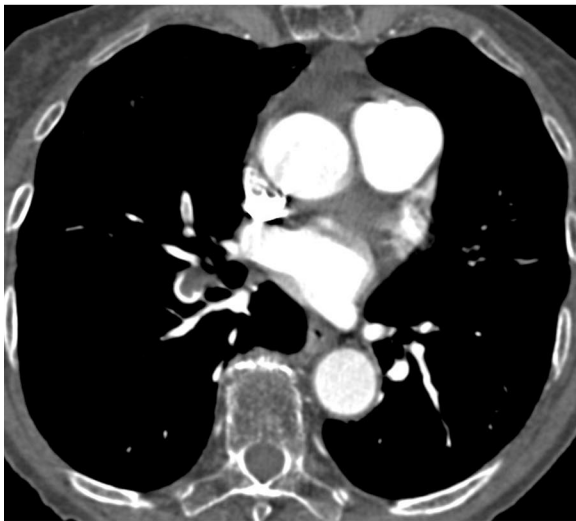
Streak Artifact.—Beam-hardening streak artifacts from dense contrast material within the superior vena cava are commonly seen and can overlie the right pulmonary and upper lobe arteries. This artifact can be distinguished from pulmonary embolism by recognizing its nonanatomic, poorly defined, radiating nature (Fig 26) and can be reduced by flushing the superior vena cava with saline solution using dual chamber injectors.



a.



b.

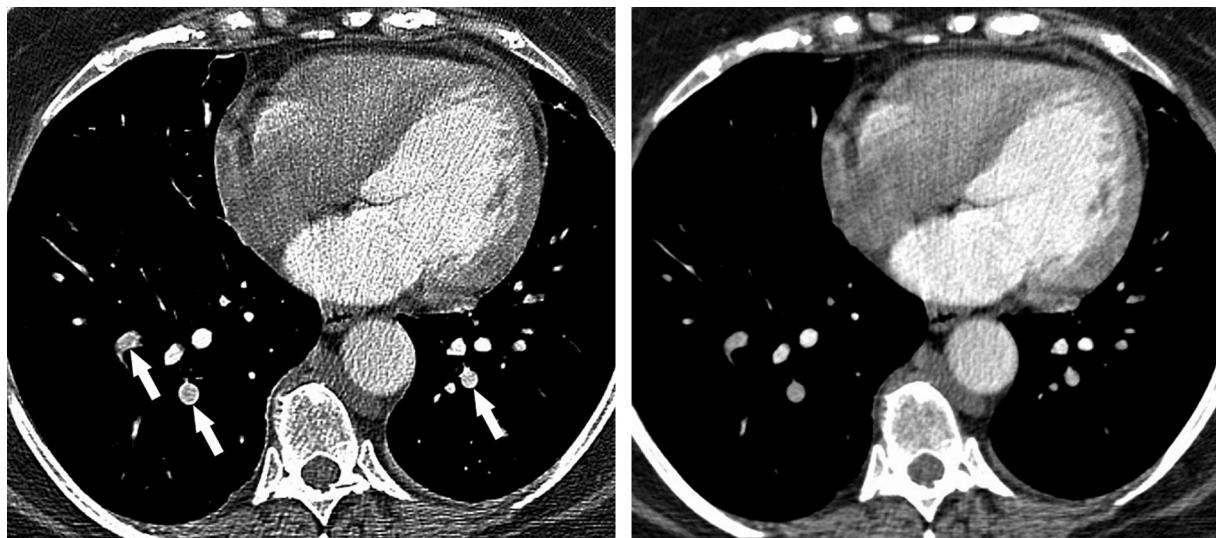


c.

Figure 25. Acute pulmonary embolism in a 59-year-old man. (a) CT scan (window width = 400 HU, window level = 40 HU) demonstrates thrombus within the right interlobar artery (arrow). (b) CT scan (window width = 552 HU, window level = 276 HU) shows acute pulmonary embolism within the medial segment of the middle lobe artery (arrow) that was missed on the image in a. The window width is equal to the mean attenuation of the main pulmonary artery plus two standard deviations, and the window level equals one-half of this value (29). (c) CT scan (window width = 700 HU, window level = 100 HU) demonstrates thrombus within the right interlobar artery and the medial segment of the middle lobe artery. Figure 25 illustrates the effect of different window settings on detection of pulmonary embolism.



Figure 26. Streak artifact in a 35-year-old woman with chest pain. CT scan shows streak artifact from dense contrast material within the superior vena cava (arrows). The artifact can be recognized by its nonanatomic, radiating nature.



a. **Figure 27.** Lung algorithm artifact in a 70-year-old woman with dyspnea. **(a)** CT scan obtained with an edge-enhancing algorithm shows a lung algorithm artifact that mimics acute pulmonary embolism (arrows). This finding is seen when viewed with mediastinal or pulmonary embolism–specific windows and manifests as a bright ring around pulmonary arteries, particularly if associated with a flow artifact. **(b)** CT scan obtained with the standard algorithm does not demonstrate this artifact. No embolism was present.

Lung Algorithm Artifact.—The lung algorithm is a high-spatial-frequency reconstruction convolution kernel used to improve the quality of images of the pulmonary vessels, bronchi, and interstitium. This algorithm can create image artifacts that appear similar to pulmonary emboli. However, these artifacts can be removed with a standard algorithm (Fig 27) (30).

Partial Volume Artifact.—Partial volume artifact is the result of axial imaging of an axially oriented vessel. An apparent filling defect that mimics acute pulmonary embolism may be identified. However, contiguous images will not demonstrate more apparent filling defects, and the margins are often not sharp. In addition, one of the contiguous images often demonstrates adjacent lung or bronchus (Fig 28). Partial volume artifact will become less of an issue with routine use of narrow detector widths.

Stair Step Artifact.—Stair step artifact consists of low-attenuation lines seen traversing a vessel on coronal and sagittal reformatted images (Fig 29) and is accentuated by cardiac and respiratory motion. This artifact can be eliminated or reduced by reconstructing the raw data with a 50%

overlap prior to three-dimensional image reconstruction. For example, when acquiring images with a 1.25-mm detector width, a set of images with an overlap of 0.625 mm should be retrospectively generated. However, when this artifact is due to cardiac or respiratory motion, overlapping reconstruction will not completely eradicate it.

Anatomic Factors

Partial Volume Averaging Effect in Lymph Nodes.—Hilar lymph nodes in the lungs can be conveniently divided into upper lobe, interlobe, middle lobe (lingular), and lower lobe groups (31,32). Knowledge of hilar lymph node anatomy assists in differentiating lymph nodes from pulmonary embolism. The most common locations of hilar lymphatic tissue are demonstrated in Figure 30. However, the location of lymph nodes and their relationship to bronchi and vessels varies among patients (32). A detector width of 5 mm may result in partial volume averaging of lymph nodes and vessel that simulates pulmonary embolism. With a 1.25-mm detector width, normal or enlarged lymphatic tissue can be more easily distinguished from acute or chronic pulmonary embolism because lymphatic tissue is extramural and the normal smooth contour of the contrast material–filled vessel is preserved (Fig 30). The review of sagittal and coronal reformatted images can help in difficult cases.



a.



b.



c.

Figure 28. Partial volume artifact in a 52-year-old woman with dyspnea. **(a)** On a 3.75-mm-thick CT scan, partial volume averaging of vessel and lung creates an artifact that mimics pulmonary embolism within the anterior segment of the left upper lobe pulmonary artery (arrow). The apparent pulmonary embolism is ill defined. **(b)** Contiguous CT scan obtained inferior to **a** demonstrates normal lung adjacent to the left upper lobe pulmonary artery. **(c)** Contiguous CT scan obtained immediately superior to **a** demonstrates a contrast material–filled pulmonary artery, a finding that confirms that the low attenuation seen in **a** was due to partial volume artifact.

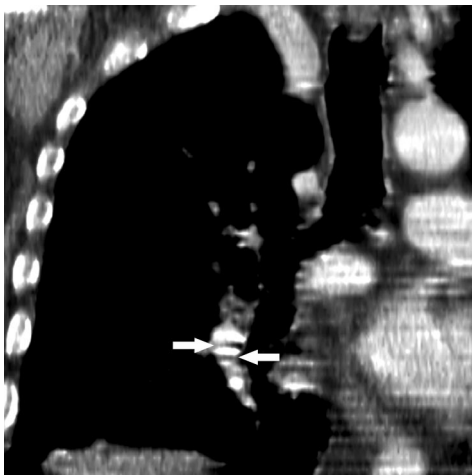


Figure 29. Stair step artifact in an 84-year-old man with dyspnea and chest pain. CT scan shows low-attenuation lines that traverse a vessel on coronal reformatted images (arrows). This artifact can be recognized by its nonanatomic nature and is easily distinguished from pulmonary embolism.

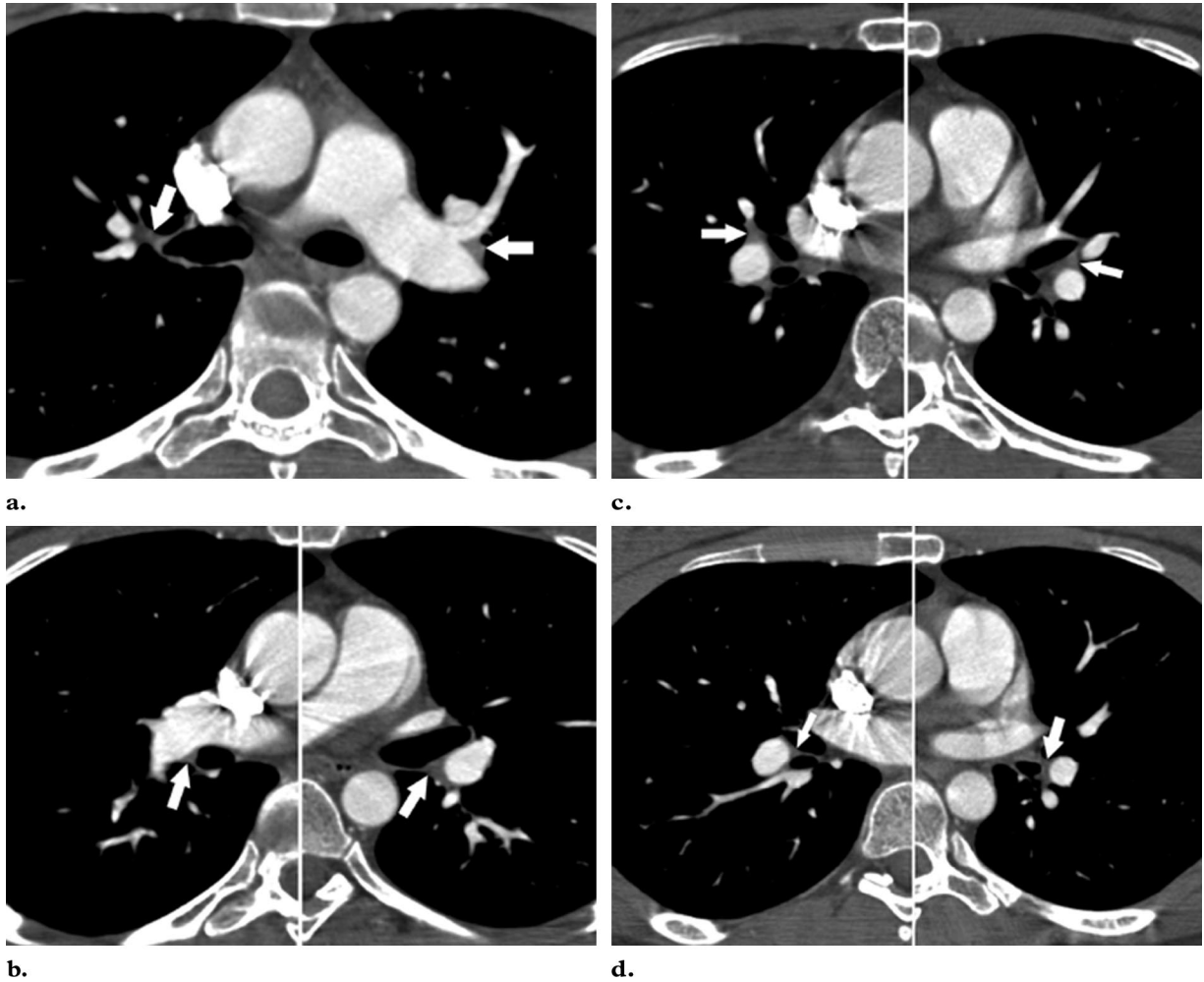


Figure 30. CT scans demonstrate normal hilar lymph nodes in both upper lobes (arrows in **a**), adjacent to the right and left interlobar arteries (arrows in **b**), in the middle lobe and lingula (arrows in **c**), and in both lower lobes (arrows in **d**).

Vascular Bifurcation.—On axial images, vascular bifurcations may simulate linear filling defects (Fig 31). Sagittal and coronal reformatted images can help identify these normal anatomic structures (17).

Misidentification of Veins.—False filling defects may be demonstrated within the pulmonary veins. These entities are caused by poor mixture of unenhanced blood and contrast material or if CT is performed too soon after the start of contrast material injection (Fig 32). This pitfall can be avoided by observing veins to the level of the right atrium on contiguous images (33). Generally, arteries course adjacent to the corresponding

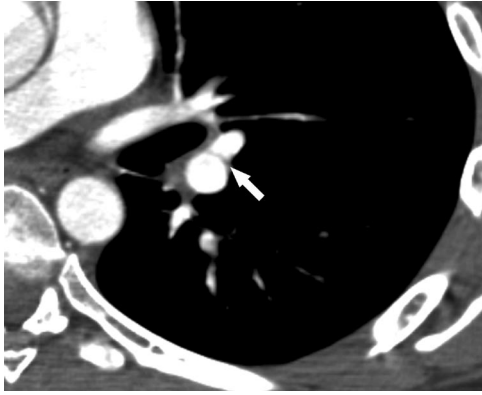


Figure 31. CT scan shows the vascular bifurcation between the left lower lobe and lingular arteries as a curved line surrounded by contrast material (arrow). Contiguous images demonstrated the true nature of this finding.



Figure 33. Mucus plugs in an 83-year-old woman with dyspnea. CT scan shows mucus plugs (arrows), which can mimic acute pulmonary embolism. The posterobasal segment of the right lower lobe bronchus is dilated as well as mucus filled. Identification of the normal accompanying pulmonary arteries (arrowheads) allows the correct interpretation of this finding.

bronchi, with the exception of the apical-posterior segment of the left upper lobe and the lingular arteries, which may course independently for a short distance before rejoining the bronchi (34).

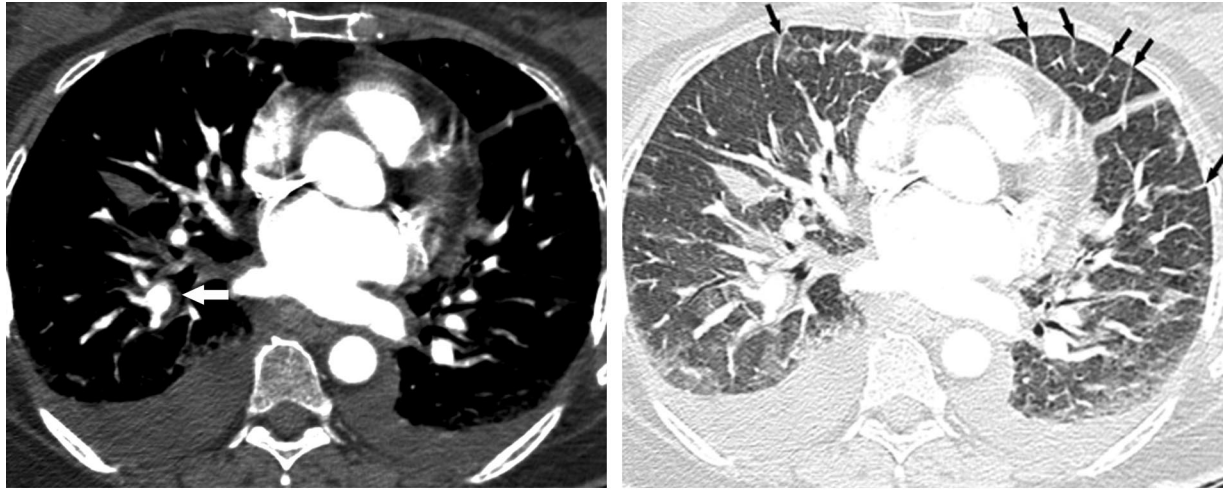


Figure 32. CT scan shows unenhanced pulmonary veins (arrows), which can mimic complete occlusive pulmonary embolism. However, this pitfall can be recognized by observing veins on contiguous images to the level of the right atrium.

Pathologic Factors

Mucus Plug.—A mucus plug within a bronchus, which may also demonstrate peripheral wall enhancement related to inflammation, can mimic acute pulmonary embolism (Fig 33). The normal-appearing contrast material-filled accompanying pulmonary artery should provide a clue regarding this artifact. In addition, viewing the bronchus on contiguous images will demonstrate the true nature of the artifact.

Perivascular Edema.—Edema caused by raised left atrial pressure can produce peribronchovascular interstitial thickening, which mimics chronic pulmonary embolism at CT pulmonary angiography. Accompanying CT findings in heart failure include diffuse ground-glass attenuation, interlobular septal thickening and diffuse peribronchovascular interstitial thickening, and bilateral pleural effusions (Fig 34).



a. **b.**
Figure 34. Left-sided heart failure in a 56-year-old woman with dyspnea. **(a)** CT scan shows peribronchovascular interstitial thickening caused by perivascular edema (arrow), a finding that can mimic chronic pulmonary embolism. **(b)** CT scan (lung window) demonstrates the accompanying findings of diffuse peribronchovascular thickening, ground-glass attenuation, smooth interlobular septal thickening (arrows), and bilateral pleural effusions. These findings indicate the true nature of the patient's condition.

Localized Increase in Vascular Resistance.

—A focal increase in vascular resistance can result from lung consolidation or atelectasis, is a cause of indeterminate CT pulmonary angiography, and can cause misdiagnosis of pulmonary embolism (Fig 35) (35). The unenhanced or poorly enhanced blood within the affected vessel may mimic pulmonary embolism. Recognition of this phenomenon is important because the unenhanced vessel may be normal or the poor contrast enhancement may obscure thrombus. A region-of-interest measurement may be helpful if the attenuation is greater than 78 HU (28). Further imaging may be necessary, consisting of either repeat CT pulmonary angiography with an increased delay or pulmonary angiography.

Pulmonary Artery Stump In Situ Thrombosis.—Virchow (36) postulated that thrombus formation is caused by vessel injury, disturbance of blood flow, and hypercoagulability. All three factors are present in patients who have undergone resection for lung cancer. On occasion, intravascular thrombosis is identified in a pulmonary artery stump. The criteria for in situ thrombus include *(a)* thrombus at the surgical site only (Fig 36) and *(b)* the absence of other pulmonary artery thrombi remote from the stump site (37).

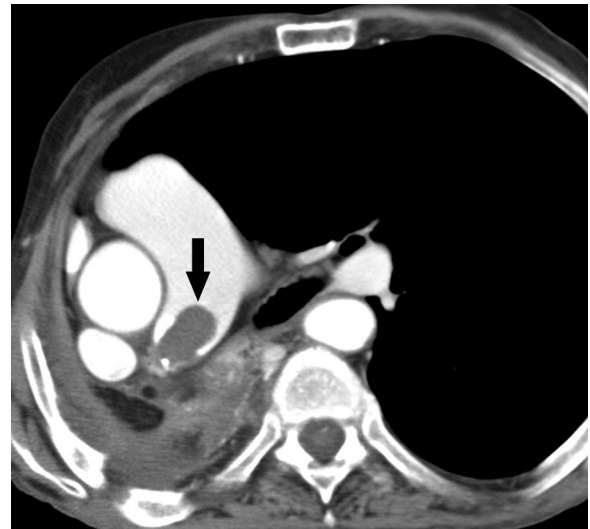


Figure 36. Pulmonary artery stump in situ thrombosis in a 69-year-old man who had undergone right pneumonectomy for lung cancer. CT scan demonstrates pulmonary artery stump in situ thrombosis that affects the right pulmonary artery (arrow).

Primary Pulmonary Artery Sarcoma.—A primary pulmonary artery sarcoma is an uncommon cause of an intraluminal arterial filling defect. These intravascular tumors manifest as unilateral, lobulated, heterogeneously enhancing masses at CT (38,39). They may demonstrate vascular distention and local extravascular spread

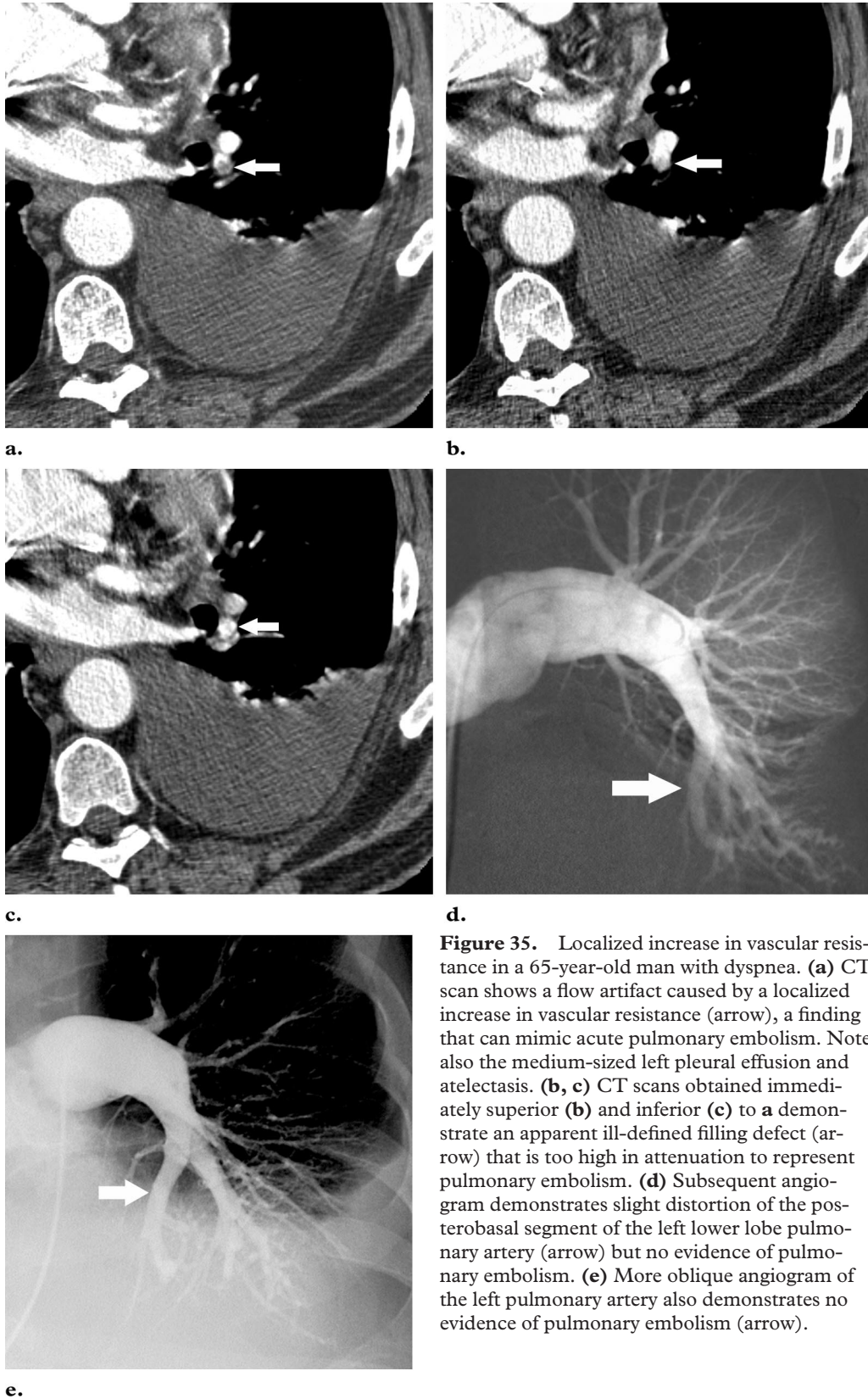


Figure 35. Localized increase in vascular resistance in a 65-year-old man with dyspnea. **(a)** CT scan shows a flow artifact caused by a localized increase in vascular resistance (arrow), a finding that can mimic acute pulmonary embolism. Note also the medium-sized left pleural effusion and atelectasis. **(b, c)** CT scans obtained immediately superior **(b)** and inferior **(c)** to **a** demonstrate an apparent ill-defined filling defect (arrow) that is too high in attenuation to represent pulmonary embolism. **(d)** Subsequent angiogram demonstrates slight distortion of the posterobasal segment of the left lower lobe pulmonary artery (arrow) but no evidence of pulmonary embolism. **(e)** More oblique angiogram of the left pulmonary artery also demonstrates no evidence of pulmonary embolism (arrow).

(40). Unlike acute pulmonary embolism, both pulmonary artery sarcoma and chronic pulmonary embolism demonstrate enhancement (Fig 37) (28,38,39); however, pulmonary artery sarcoma is lobulated and forms acute angles with the vessel wall (Fig 37), whereas chronic pulmonary embolism forms obtuse angles (Fig 12).

Tumor Emboli.—Intravascular tumor emboli can manifest as large, acute pulmonary emboli that produce acute pulmonary hypertension by occluding main, lobar, or segmental pulmonary arteries. More commonly, tumor emboli are small and occlude subsegmental arteries and arterioles, leading to progressive dyspnea and subacute pulmonary hypertension (41). Tumor emboli are often associated with recent and organizing thrombi (41,42). Large tumor emboli, a rare cause of intravascular filling defects, result from direct invasion of the inferior vena cava or its major branches by hepatoma, renal cell carcinoma, or choriocarcinoma (42). In a review of microscopic pulmonary tumor emboli associated with dyspnea, Kane et al (41) found that carcinomas of the prostate gland and breast were the most common causes, followed by hepatoma, then carcinomas of the stomach and pancreas (41). Manifestations of tumor emboli at CT include (a) large emboli in the main, lobar, and segmental pulmonary arteries that cause filling defects that mimic acute pulmonary thromboembolism (Fig 38), (b) small tumor emboli that affect subsegmental arteries and produce vascular dilatation and beading that increases in size over time (Fig 39) (43), and (c) small tumor emboli that affect secondary pulmonary lobule arterioles and have a tree-in-bud appearance (Fig 40) (44,45).

Conclusions

The radiologist needs to determine the quality of a CT pulmonary angiographic study and whether pulmonary embolism is present. If the quality of the study is poor, the radiologist should identify which pulmonary arteries are rendered indeterminate and whether additional imaging is necessary.

References

1. Anderson FA Jr, Wheeler B, Goldberg RJ, et al. A population-based perspective of the hospital incidence and case fatality rates of deep vein thrombosis and pulmonary embolism: the Worcester DVT study. *Arch Intern Med* 1991; 151:933-938.
2. Giuntini C, Ricco GD, Marini C, et al. Pulmonary embolism: epidemiology. *Chest* 1995; 107(suppl): 3S-9S.

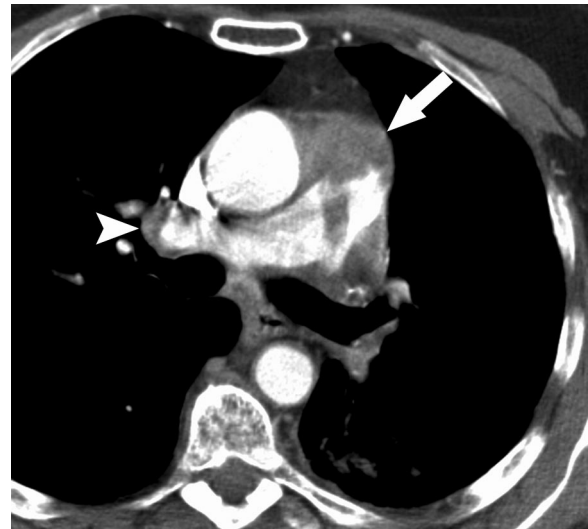
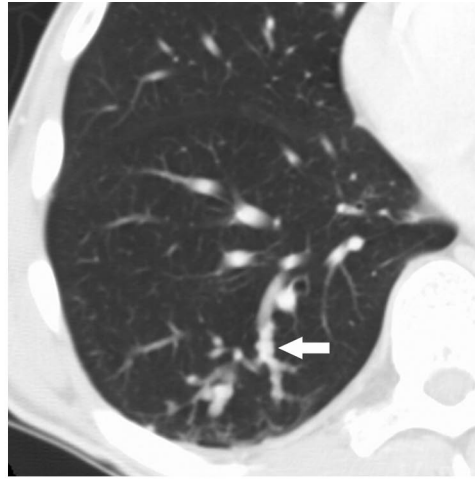


Figure 37. Pulmonary artery sarcoma in a 65-year-old woman with dyspnea. Contrast-enhanced CT scan shows a heterogeneously enhancing, lobulated mass within the main pulmonary artery (arrow). A metastatic deposit is noted within the right pulmonary artery (arrowhead).

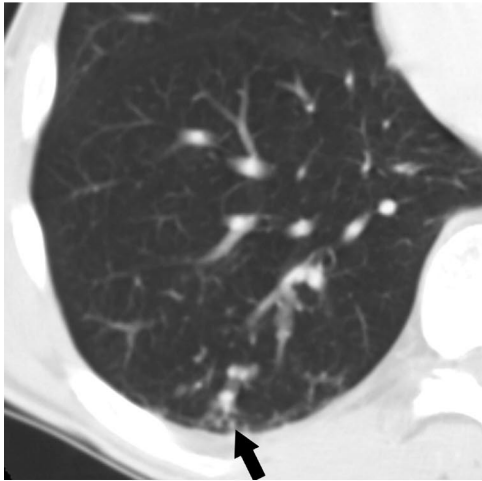
3. Brown MD, Rowe BH, Reeves MJ, Birmingham JM, Goldhaber SZ. The accuracy of the enzyme-linked immunosorbent assay D-dimer test in the diagnosis of pulmonary embolism: a meta-analysis. *Ann Emerg Med* 2002; 40:133-134.
4. Value of ventilation/perfusion scan in acute pulmonary embolism: results of the Prospective Investigation of Pulmonary Embolism Diagnosis (PIOPED)—the PIOPED investigators. *JAMA* 1990; 263:2753-2759.
5. Borris LC, Christiansen HM, Lassen MR, Olsen AD, Schutt P. Comparison of real-time B-mode ultrasonography and bilateral ascending phlebography for detection of postoperative deep vein thrombosis following elective hip surgery: the Venous Thrombosis Group. *Thromb Haemost* 1989; 61:363-365.
6. Rathbun SW, Raskob GE, Whitsett TL. Sensitivity and specificity of helical computed tomography in the diagnosis of pulmonary embolism: a systematic review. *Ann Intern Med* 2000; 132:227-232.
7. Schluger N, Henschke C, King T, et al. Diagnosis of pulmonary embolism at a large teaching hospital. *J Thorac Imaging* 1994; 9:180-184.
8. Henschke CI, Mateescu I, Yankelevitz DF. Changing practice patterns in the workup of pulmonary embolism. *Chest* 1995; 107:940-945.
9. Kelley MA, Carson JL, Palevsky HI, et al. Diagnosing pulmonary embolism: new facts and strategies. *Ann Intern Med* 1991; 114:300-306.
10. Cheely R, McCartney WH, Perry JR, et al. The role of noninvasive tests versus pulmonary angiography in the diagnosis of pulmonary embolism. *Am J Med* 1981; 70:17-22.
11. Stein PD, Anthanasoulis C, Alavi A, et al. Complications and validity of pulmonary angiography in acute pulmonary embolism. *Circulation* 1992; 85:462-468.



38.



39.



40.

Figures 38–40. (38) Tumor embolus in a 78-year-old woman with dyspnea and endometrial stromal sarcoma that invaded the inferior vena cava. CT scan shows a large tumor embolus within the right lower lobe pulmonary artery (arrow). (39, 40) Tumor emboli in a 60-year-old man with dyspnea and primary renal cell carcinoma. (39) CT scan shows tumor emboli that manifest as vascular dilatation and beading of subsegmental arteries of the postero-basal segment of the right pulmonary artery (arrow). (40) CT scan shows tumor emboli with a tree-in-bud appearance within secondary pulmonary lobule arterioles (arrow). Tumor emboli rarely have such an appearance at CT.

12. Wittram C, Meehan MJ, Halpern EF, et al. Trends in thoracic radiology over a decade at a large academic medical center. *J Thorac Imaging* 2004; 19:164–170.
13. Remy-Jardin M, Remy J, Cauvain O, et al. Diagnosis of central pulmonary embolism with helical CT: role of two-dimensional multiplanar reformations. *AJR Am J Roentgenol* 1995; 165:1131–1138.
14. Loud PA, Katz DS, Bruce DA, et al. Deep venous thrombosis with suspected pulmonary embolism: detection with combined CT venography and pulmonary angiography. *Radiology* 2001; 219:498–502.
15. Gottschalk A, Stein PD, Goodman LR, Sostman HD. Overview of prospective investigation of pulmonary embolism diagnosis II. *Semin Nucl Med* 2002; 32:173–182.
16. Ghaye B, Remy J, Remy-Jardin M. Non-traumatic thoracic emergencies: CT diagnosis of acute pulmonary embolism—the first 10 years. *Eur Radiol* 2002; 12:1886–1905.
17. Washington L, Goodman LR, Gonyo MB. CT for thromboembolic disease. *Radiol Clin North Am* 2002; 40:751–771.
18. Coche EE, Muller NL, Kim K, et al. Acute pulmonary embolism: ancillary findings at spiral CT. *Radiology* 1998; 207:753–758.
19. Contractor S, Maldjian PD, Sharma VK, et al. Role of helical CT in detecting right ventricular dysfunction secondary to acute pulmonary embolism. *J Comput Assist Tomogr* 2002; 26:587–591.
20. Wu AS, Pezzullo JA, Cornan JJ, Hou DD, Mayo-Smith WW. CT pulmonary angiography: quantification of pulmonary embolus as a predictor of patient outcome—initial experience. *Radiology* 2004; 230:831–835.
21. Gosselin MV, Rubin GD, Leung AN, et al. Un-suspected pulmonary embolism: prospective detection on routine helical CT scans. *Radiology* 1998; 208:209–215.
22. Kanne JP, Gotway MB, Thoongsuwan N, et al. Six cases of acute central pulmonary embolism revealed on unenhanced multidetector CT of the chest. *AJR Am J Roentgenol* 2003; 180:1661–1664.
23. Edwards PD, Bull RK, Coulden R. CT measurement of main pulmonary artery diameter. *Br J Radiol* 1998; 71:1018–1020.
24. Baque-Juston MC, Wells AU, Hansell DM. Pericardial thickening or effusion in patients with pulmonary artery hypertension: a CT study. *AJR Am J Roentgenol* 1999; 172:361–364.

25. Schoepf UJ, Holzkecht N, Helmberger T, et al. Subsegmental pulmonary emboli: improved detection with thin-collimation multi-detector row spiral CT. *Radiology* 2002; 222:483-490.
26. Gotway MB, Patel RA, Webb WR. Helical CT for the evaluation of suspected acute pulmonary embolism: diagnostic pitfalls. *J Comput Assist Tomogr* 2000; 24:267-273.
27. Gosselin MV, Rassner UA, Thieszen SL, et al. Contrast dynamics during CT pulmonary angiogram: analysis of an inspiration associated artifact. *J Thorac Imaging* 2004; 19:1-7.
28. Wittram C, Maher MM, Halpern E, et al. The Hounsfield unit values of acute and chronic pulmonary emboli (abstr). In: Radiological Society of North America scientific assembly and annual meeting program. Oak Brook, Ill: Radiological Society of North America, 2003; 678.
29. Brink JA, Woodard PK, Horesh L, et al. Depiction of pulmonary emboli with spiral CT: optimization of display window settings in a porcine model. *Radiology* 1997; 204:703-708.
30. Swensen SJ, Morin RL, Aughenbaugh GL, et al. CT reconstruction algorithm selection in the evaluation of solitary pulmonary nodules. *J Comput Assist Tomogr* 1995; 19:932-935.
31. Sone S, Higashiha T, Morimoto S, et al. CT anatomy of hilar lymphadenopathy. *AJR Am J Roentgenol* 1983; 140:887-892.
32. Remy-Jardin M, Remy J, Artuad D, et al. Spiral CT of pulmonary embolism: technical considerations and interpretive pitfalls. *J Thorac Imaging* 1997; 12:103-117.
33. Beigelman C, Chartrand-Lefebvre C, Howarth NO, Grenier P. Pitfalls in diagnosis of pulmonary embolism with helical CT angiography. *AJR Am J Roentgenol* 1998; 171:579-585.
34. Kuzo RS, Goodman LR. CT evaluation of pulmonary embolism: technique and interpretation. *AJR Am J Roentgenol* 1997; 169:959-965.
35. Goodman LR, Curtin JJ, Mewissen MW, et al. Detection of pulmonary embolism in patients with unresolved clinical and scintigraphic diagnosis: helical CT versus angiography. *AJR Am J Roentgenol* 1995; 164:1369-1374.
36. Virchow R. Cellular pathology as based upon physiological and pathological histology. London, England: Churchill, 1860.
37. Wechsler RJ, Salazar AM, Gessner AJ, et al. CT of in situ vascular stump thrombosis after pulmonary resection for cancer. *AJR Am J Roentgenol* 2001; 176:1423-1425.
38. Chow B, Wittram C, Lee VW. Unilateral absence of pulmonary perfusion mimicking pulmonary embolism. *AJR Am J Roentgenol* 2001; 176:712.
39. Cox JE, Chiles C, Aquino SL, et al. Pulmonary artery sarcomas: a review of clinical and radiologic features. *J Comput Assist Tomogr* 1997; 21:750-755.
40. Yi CA, Lee KS, Choe YH, et al. Computed tomography in pulmonary artery sarcoma: distinguishing features from pulmonary embolic disease. *J Comput Assist Tomogr* 2004; 28:34-39.
41. Kane RD, Hawkins HK, Miller JA, et al. Microscopic pulmonary tumor emboli associated with dyspnea. *Cancer* 1975; 36:1473-1482.
42. Winterbauer RH, Elflein IB, Ball WC Jr. Incidence and clinical significance of tumor embolization to the lungs. *Am J Med* 1968; 45:271-290.
43. Shepard JA, Moore EH, Templeton PA, McLoud TC. Pulmonary intravascular tumor emboli: dilated and beaded peripheral pulmonary arteries at CT. *Radiology* 1993; 187:797-801.
44. Tack D, Nollevaux MC, Gevenois PA. Tree-in-bud pattern in neoplastic pulmonary emboli. *AJR Am J Roentgenol* 2001; 176:1421-1422.
45. Han D, Lee KS, Franquet T, et al. Thrombotic and nonthrombotic pulmonary arterial embolism: spectrum of imaging findings. *RadioGraphics* 2003; 23:1521-1539.